High-Pressure NMR Study of the Dissociation of Arc Repressor†

Xiangdong Peng and Jiri Jonas*

School of Chemical Sciences, University of Illinois, Urbana, Illinois 61801

Jerson L. Silva*

Departamento de Bioquimica, Instituto de Ciencias Biomedicas, Universidade Federal do Rio de Janeiro, 21910 Rio de Janeiro, RJ, Brazil

Received February 16, 1994; Revised Manuscript Received May 5, 1994®

ABSTRACT: Different denatured states of Arc repressor were characterized by one-dimensional and two-dimensional NMR and by fluorescence spectroscopy. Increasing pressure promoted sequential changes in the structure of Arc repressor: from the native dimer through a predissociated state to a denaturated molten globule monomer. A compact state (molten globule) of Arc repressor was obtained in the dissociation of Arc repressor by pressure whereas high temperature and urea induced dissociation and unfolding to less structured conformations. The NMR spectra of the monomer under pressure (up to 5.0 kbar) are typical of a molten globule, and they are considerably different from those of the native dimer and the thermally or chemically denatured monomer. The substantial line broadening and overlap of many resonances in the NMR spectra at high pressures indicate that there is interconversion between a number of different conformations of the molten globule at an intermediate exchange rate. The two-dimensional NOE spectra show that the pressure-denatured monomer retains substantial secondary structure. The presence of NOEs in the β-sheet region in the dissociated state suggests that the intersubunit β-sheet (residues 6–14) in the native-dimer is replaced by an intramonomer β-sheet. Changes in 2D NMR spectra prior to dissociation indicate the existence of a predissociated state that may represent an intermediate in the folding and subunit association pathway of Arc repressor.

The stability of proteins has been extensively studied by temperature and chemical perturbations [for a review, see Dill and Shortle (1991)]. High temperature changes both the energy content and the volume of a system. Since proteins are flexible polymers folded into three-dimensional structures which are stabilized by interactions of strengths not much larger than the thermal energy, the internal interactions of proteins are changed by temperature in ways that cannot be easily foreseen (Silva & Weber, 1993). Similarly, the effects of denaturants on proteins are difficult to interpret because they also modify the chemical potential of proteins in unpredictable ways on binding to multiple sites with different affinities. The use of hydrostatic pressure to perturb protein structure is more recent and less frequent than the use of heat and chemical agents (Zipp & Kauxmann, 1973; Heremans, 1982; Weber & Drickamer, 1983; Silva & Weber, 1993). However, the effects of pressure are easier to interpret because pressure perturbs internal interactions exclusively by changing the distances between the components, while the total energy of the system remains almost constant. Pressure studies on single-polypeptide proteins suggest that at high pressure the protein is infiltrated by water. Because of the higher compressibility, the weakest bonds, those due to dispersion forces between the amino acid residues, are destabilized first (Weber, 1993) and are replaced by protein–water interactions.

A recent major advance in the study of protein folding has been the discovery of intermediates in the folding pathways. Clearly, an important research objective is to find ways to stabilize and to characterize the folding intermediates. Examples of intermediate states and methods to characterize their structure have been reported recently (Kim & Baldwin, 1990; Dill & Shortle, 1991). Studies on several stable folding intermediates indicate that they have compact structures, termed molten globules (Ohgushi & Wada, 1983), having similar secondary structures to the native states but disordered tertiary structures (Ptitsyn, 1987). The association of subunits is an additional problem in the case of oligomeric proteins (Jaenicke, 1987, 1991); however, it is expected that the interactions between the residues in the interface between subunits are governed by the same rules that determine the folding of a single-chain protein.

Arc repressor is a small, DNA binding dimeric protein, consisting of 53 amino acid residues (M_r = 13 000). It represses transcription from the P_{ant} promoter of *Salmonella* bacteriophage P22 (Susskind, 1980; Sauer et al., 1983; Vershon et al., 1985). Arc repressor belongs to a family of proteins that have an antiparallel β-sheet as the interfacial DNA binding motiff (Knight et al., 1989; Breg et al., 1990; Phillips, 1991). A tertiary structure model for Arc repressor has been proposed (Breg et al., 1990) based upon homology between the Arc repressor and the *Escherichia coli* Met repressor and on two-dimensional NMR data (Breg et al., 1989; Zagorski et al., 1989). This model consists of an intertwined dimer in which residues 8–14 of each monomer participate in the formation of an antiparallel β-sheet. Arc repressor dimer dissociates reversibly into subunits with increasing pressure, at fixed protein concentration, or with dilution, at constant pressure (Silva et al., 1992). The Arc repressor monomer obtained by compression is compact and, as measured by its rotational diffusion, has a much smaller hydrodynamic radius than that of Arc repressor denatured by urea. The dissociated

† This work was supported by the National Institutes of Health under Grant PHS 1 R01 GM42452 to J.J., by Conselho Nacional de Desenvolvimento Cientifico e Tecnologico (CNPq) to J.L.S., and by the National Institutes of Health under Grant PHS GM-11223 to G. Weber. J.L.S. is a John Simon Guggenheim Fellow.

* Authors to whom correspondence should be addressed.

® Abstract published in *Advance ACS Abstracts,* June 15, 1994.

0006-2960/94/0433-8323$04.50/0

Arc repressor exposes a nonpolar core and binds bis(8-anilinonaphthalene-1-sulfonate) strongly (Silva et al., 1992). Thus, the properties of the Arc repressor dissociated by pressure agree with the characteristic properties of a molten globule (Goto & Fink, 1989; Ptytsin, 1987; Ptytsin et al., 1990). The previous fluorescence studies clearly show that the pressure-dissociated form of the Arc repressor retains significant three-dimensional structure in contrast to the urea-denatured or temperature-denatured forms of the protein. A preliminary high-pressure NMR study from our laboratory suggests that the pressure-induced molten globule state of Arc repressor monomer adopts a β-strand, γ-turn, β-strand structure in the residue 8–14 region (Peng et al., 1993).

Nuclear magnetic resonance is a powerful tool for the investigation of protein structure and the dynamics of protein folding intermediates (Roder, 1989). High-pressure NMR techniques have been extensively used to study the dynamic structure of liquids (Jonas, 1982, 1987). More recently, high-pressure, high-resolution NMR techniques including advanced 2D techniques have been used to investigate pressure effects on protein structure and reaction mechanisms (Jonas & Jonas, 1994). In addition to the preliminary NMR study on the pressure dissociation of Arc repressor (Peng et al., 1993), high-resolution NMR techniques were used to investigate the pressure-induced reversible unfolding of lysozyme (Samarasinghe et al., 1992) and the cold denaturation of ribonuclease A (Peng, Zhang, and Jonas, unpublished results). The results of the effects of amino acid substitution on pressure unfolding on staphylococcal nuclease (Royer et al., 1993) demonstrated the great potential of site-directed mutagenesis combined with high-pressure NMR in studies of protein stability.

The present study using high-pressure, high-resolution NMR techniques including 2D techniques is a continuation of an earlier study of Arc repressor by fluorescence techniques (Silva et al., 1992) and our preliminary NMR experiments (Peng et al., 1993). This study had several goals: first, using 1D and 2D NMR techniques to determine how different is the pressure-dissociated Arc repressor monomer from the monomer forms obtained by thermal or urea denaturation; second, to provide experimental evidence for the existence of a pressure-induced predissociated state of Arc repressor which was suggested by our preliminary NMR experiments; third, to partially characterize the structure of the predissociated state and the molten globule monomer state of Arc repressor. Finally, we also wanted to show that pressure is a more easily controlled and less drastic perturbation of protein structure than thermal or chemical denaturation.

MATERIALS AND METHODS

Sample Preparation. Arc repressor was expressed in *E. coli* and purified as described previously (Vershon et al., 1985, 1986). The labile protons were exchanged by repeated lyophilization and dissolution in D_2O. All samples were dissolved in a deuterated buffer containing 50 mM Tris (pD 7.5)/100 mM NaCl. The sample concentrations ranged from 0.3 to 1.5 mM. All chemical shifts were referenced to an internal standard of sodium 3-(trimethylsilyl)tetradeuteriopropionate.

NMR Spectroscopy. All NMR spectra were recorded on a GE GN-300 spectrometer system. The spectrometer is equipped with an Oxford Instruments Co. superconducting 7.0-T magnet and a GE/Nicolet 1280 computer. The home-built high-pressure, high-resolution NMR probe (Jonas et al., 1993) was used for both the temperature and pressure measurements. The pressure-transmitting fluid, CS_2, was used inside the titanium high-pressure vessel, and the sample was isolated from CS_2 by a movable Teflon piston. The temperature was controlled by circulating a mixture of ethylene glycol and water around the high-pressure vessel, and was measured with a copper–constantan thermocouple inside the vessel. The temperature range studied was from 10 to 70 °C, and the pressure range from 1 bar up to 5 kbar at 20 °C.

1D NMR experiments were performed using the following spectrometer parameters: 16K data points in the FID and a spectral width of 5 kHz; 60° excitation pulse with an acquisition delay of 2 s. For the 2D NMR experiments, both phase-sensitive COSY (Bax et al., 1981), DQF-COSY (Rance et al., 1984; Shaka & Freeman, 1983), TOCSY (Braunschweiler & Ernst, 1983; Bax & Davis, 1985), and NOESY or exchange-correlated spectra (States et al., 1982; Macura et al., 1982; Rance et al., 1985) were recorded with a spectral width of 4 kHz, 1–2 s of recycle delay, and two dummy scans before each FID. A time domain data set of 412 × 2K points were recorded and Fourier-transformed in both dimensions after multiplication by a sine bell window function shifted by 0–45° and zero-filling prior to the second Fourier transformation. The final data set consists of 1K × 1K real data points.

High-Pressure Fluorescence Spectroscopy. The high-pressure cell has been described by Paladini and Weber (1981). Fluorescence spectra were recorded with a computer-controlled photon-counting spectrofluorometer. ISS Software (Champaign, IL) was used for data acquisition and analysis. Fluorescence spectra at pressure P were quantified by specifying the center of spectral mass, $\langle \upsilon_P \rangle$, in wavenumbers ($cm^{-1}$):

$$\langle \upsilon_P \rangle = \Sigma \upsilon_i F_i / \Sigma F_i \qquad (1)$$

where F_i stands for the fluorescence emitted at wavenumber υ_i. The summation is carried out over the range of appreciable values of F. The degree of dissociation (α_P) is related to $\langle \upsilon_P \rangle$ by the expression:

$$\alpha_P = [1 + Q(\langle \upsilon_P \rangle - \langle \upsilon_F \rangle)/(\langle \upsilon_I \rangle - \langle \upsilon_P \rangle)] - 1 \qquad (2)$$

where Q is the ratio of the quantum yields of dissociated and associated forms, $\langle \upsilon_P \rangle$ is the center of spectral mass at pressure P, and $\langle \upsilon_F \rangle$ and $\langle \upsilon_I \rangle$ are the corresponding quantities for dissociated and associated forms (Silva et al., 1986, 1989).

Structure Generation. The structures of the β-sheet region of the Arc repressor in the predissociated state and the molten globule state were obtained from restrained molecular dynamics calculations and energy minimizations starting from the initial structure and modifying the antiparallel dimer structure provided by Prof. R. Kaptein. The experimental NOEs are classified as strong, medium, and weak NOEs corresponding to distance ranges of approximately 1.8–2.7, 1.8–3.3, and 1.8–5.0 Å, respectively. The restrained molecular dynamics calculation was used to produce 3D structures consistent with distance and torsion restraints by taking into account both bonded and nonbonded interactions while the energy minimization calculation was used to further optimize the 3D structure by keeping bond lengths and angles fixed and varying the torsion angles. The structures were obtained for several cycles of restrained molecular dynamics calculations followed by energy minimizations. Calculations were carried out on a Silicon Graphics IRIS Indigo Elan workstation using Insight II and Discover programs.

During the dynamics calculations, 2000 steps at a temperature of 300 K were used. The force constants for NOE distance and dihedral angle terms were 50 and 100 kcal/mol,

respectively. In the minimization, the CVFF force field and the NMR restraints were used, and all force constants were scaled to 1.0. The converged structures were subjected to 200 iterations of steepest descent and 2000 iterations of conjugate gradient minimization to reduce repulsive nonbonded interactions.

Several starting structures of the predissociated antiparallel β-sheets were obtained by modifying the relative positions of the two β-sheets so that the distances between the α-protons of Gln9/Arg13, Gln9/Trp14 were within 5 Å simultaneously. The experimental NOEs between the α-protons of Gln9/Arg13, Gln9/Trp14 (from two subunits) and Met7/Trp14 (within one subunit) were all classified as medium NOEs corresponding to a distance range of 1.8–3.3 Å. The starting structure of the molten globule γ-turn was obtained by modifying the β-sheet structure using dihedral angles (Nemethy & Printz, 1972) for the γ-turn and distance restraints between α-protons of Gln9 and Arg13. The experimental NOEs between the α-protons of Gln9 and Arg13 (from two subunits) were classified as strong NOEs corresponding to a distance range of 1.8–2.7 Å. The structures of both the predissociated state and molten globule state shown are the average of 10 structures calculated, respectively.

RESULTS AND DISCUSSION

Pressure-, Temperature-, and Urea-Denatured States. The structure of the Arc repressor based on the NMR data (Breg et al., 1990) contains an intertwined dimer, in which residues 8–14 of each subunit participate in the formation of an antiparallel β-sheet. The two α-helices in each subunit also have substantial intersubunit interactions. It can be argued that the intersubunit interactions are as important as the intrasubunit interactions for the maintenance of the native conformation of the Arc repressor, therefore, it is conceivable that the monomers would lose most of their structure when separated from each other. Conformational changes in conjunction with dissociation of the Arc repressor were first observed on denaturation by guanidine (Bowie & Sauer, 1989). Large conformational changes were detected when the subunits were separated by hydrostatic pressure, but some residual structure remained (Silva et al., 1992).

Each Arc repressor subunit contains a single tryptophan that is located at position 14 in the interface between subunits (Breg et al., 1990; Silva et al., 1992). The low polarity of the environment of Trp14, when Arc repressor is in the dimeric state, results in a blue-shifted fluorescence emission. In this state, the wavelength of maximum emission is 328 nm, and the average energy of the emission (center of spectral mass) is 337.5 mm. When the protein is dissociated into monomers, Trp14 becomes exposed to the solvent, and the center of spectral mass shifts to 352.7 mm. The correlation between the emission at each pressure and the degree of dissociation has been confirmed by measurements of the hydrodynamic size by fluorescence polarization (Silva et al., 1992). Figure 1 compares the Trp spectra of the Arc repressor when dissociated by pressure, denatured by temperature, or denatured by urea. It is clear that in all three cases the polarity of the environment of Trp increases, leading to the conclusion (based on the fluorescence experiments) that there is no difference between the various denatured states.

In this study, we turned to high-resolution NMR experiments to demonstrate differences between the different denatured states. The 1D ^{1}H NMR spectra in the aromatic region (Figure 2) suggest that the conformation of the pressure-denatured Arc repressor is different from the thermal- or urea-denatured forms. Similar differences are also found in the NMR spectra for the aliphatic region (data not shown).

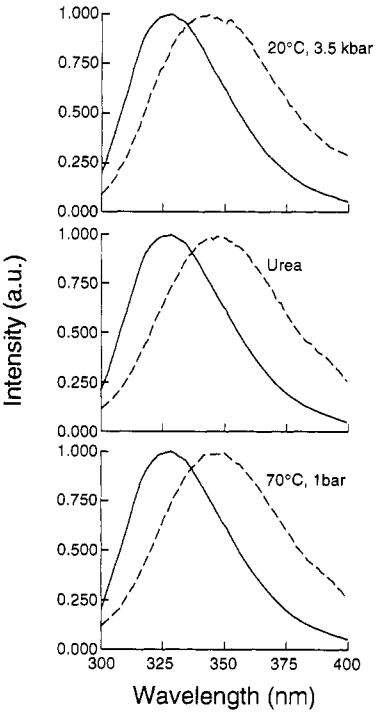

FIGURE 1: Normalized intrinsic fluorescence spectra of the Arc repressor in the native state (20 °C, 1 bar) (solid lines) and in the three unfolded states (dashed lines): (A) pressure-induced molten globule state (20 °C, 3.5 kbar); (B) urea-denatured state (20 °C, 1 bar, 7 M urea); and (C) thermally denatured state (70 °C, 1 bar).

It should be mentioned that we use the term denaturation for any major change in the conformation that leads to a disruption of the biological activity of a protein. In this case, it is legitimate to consider the dissociated state of the Arc repressor as denatured, since monomeric Arc repressor loses the high-affinity binding to DNA (Brown et al., 1990; Silva et al., 1992). The denatured state of a protein is not necessarily similar to a random coil. Our spectra of the pressure-denatured Arc repressor appear more structured than the other denatured forms. At 70 °C or in 7 M urea, Arc repressor is completely denatured and has no secondary structure (Vershon et al., 1985) as determined by circular dichroism. According to Silva et al. (1992), Arc repressor under conditions comparable to those in our experiments would begin to dissociate at about 1 kbar and completely dissociate above 3.5 kbar. Our spectra in the pressure range 1–5 kbar show substantial overlap and line broadening of many resonances. Similar spectral features have also been reported in the study of the molten globule state of guinea pig α-lactalbumin (Baum et al., 1989).

Figures 3 and 4 show the aromatic region of 1D NMR spectra at elevated pressures and temperatures, respectively. In order to demonstrate that the observed pressure effects on the NMR spectra of the Arc repressor are not due to some instrumental artifacts by operating at high pressure, we include two insets in Figure 3 which give the line width of the standard at 1 bar and 5 kbar. Clearly, excellent resolution is maintained over the entire pressure range investigated. The spectra have been assigned according to Breg et al. (1989) (see Table 1) and our 2D experiments at high pressures. It is important to point out that the spectra obtained during compression were identical to those recorded during the decompression run, indicating complete reversibility over the course of the experiments. The results obtained were reproducible for three different preparations. Inspection of Figures 3 and 4 reveals

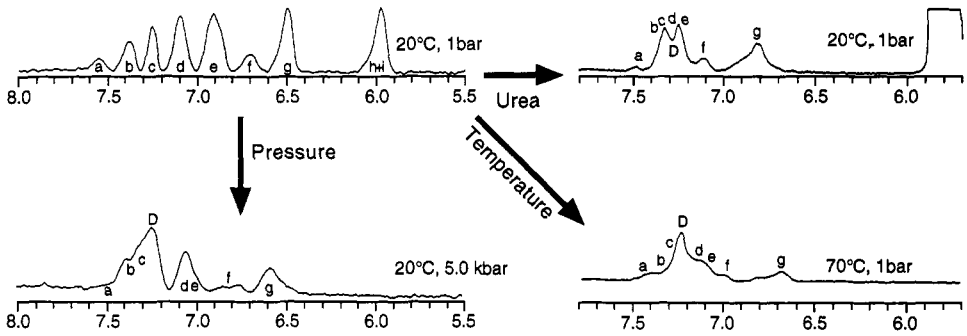

FIGURE 2: Comparison of the aromatic regions of 1D ^{1}H NMR spectra among the native state, the pressure-induced molten globule state, and the thermally denatured state of the Arc repressor.

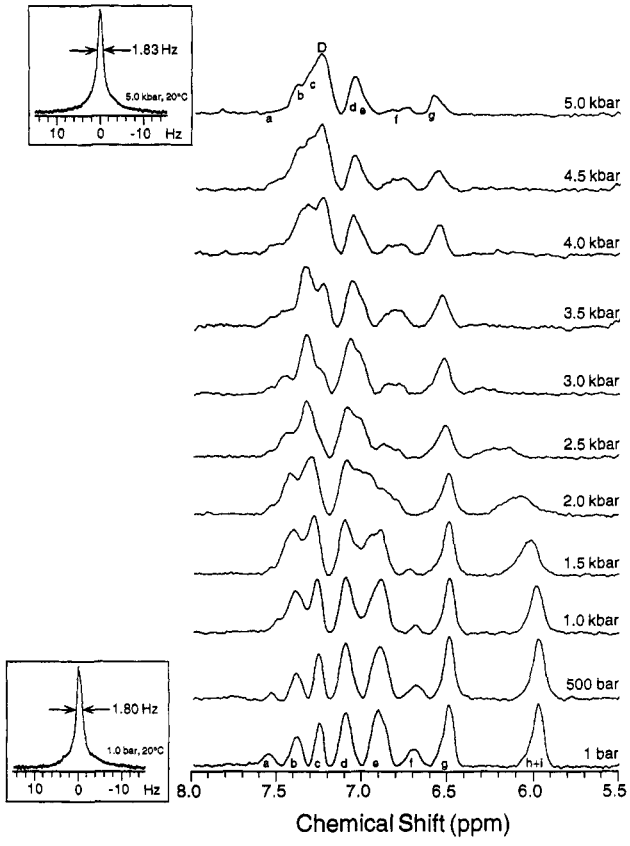

FIGURE 3: Aromatic region of the 1D ^{1}H NMR spectra of the Arc repressor at various pressures (20 °C, pD 7.5). The standard in the insets is sodium 3-(trimethylsilyl)tetradeuteriopropionate.

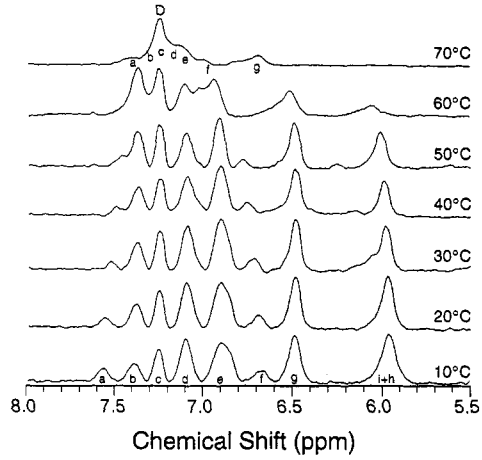

FIGURE 4: Aromatic region of the 1D ^{1}H NMR spectra of the Arc repressor at various temperatures (1 bar, pD 7.5).

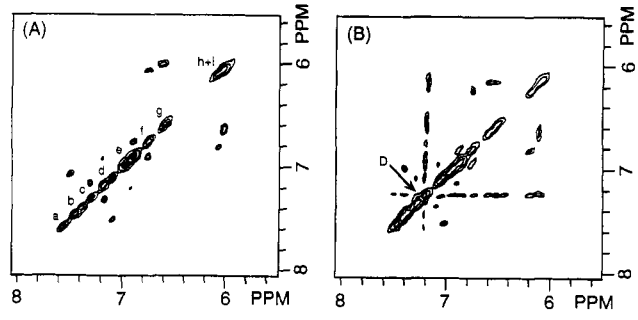

FIGURE 5: Exchange-correlated 2D spectra of the aromatic region at 1 bar, 20 °C (A), and at 2.5 kbar, 20 °C (B).

several major differences between pressure and temperature effects. Several resonances begin to merge and overlap at 1 kbar, and substantial line broadening continues up to 5 kbar. In contrast, many resonances in temperature spectra do not overlap until 60 °C.

To assign the resonance labeled D in the aromatic region of one-dimensional spectra, we performed two-dimensional exchange-correlated experiments at 1 bar and 2.5 kbar (near the midpoint of the transition between the native dimer and the molten globule monomer). The exchange cross-peaks are distinguished from NOE ones by comparing the spectrum at 2.5 kbar with that at 1 bar because only NOE cross-peaks can occur at 1 bar. Figure 5 shows the exchange-correlated spectra at 1 bar and 2.5 kbar for both the aromatic and the aliphatic regions. The cross-peaks between D and other reasonance peaks result from the interconversion of the native dimer and the molten globule monomer. COSY and DQF-COSY spectra at 2.5 kbar also support the view that the D resonance is due to dissociation of the Arc dimer (data not shown).

Table 1: Resonance Assignments for Arc Repressor in the Native State (20 °C, 1 bar)[a]

resonance	assignment	resonance	assignment
a	Trp14δ1H	f	Phe10ε2H
b	Trp14ζ2H, ε3H	g	Tyr38ε2H
c	Phe45δ2H	h	Tyr38δ2H
d	Phe45ε2H; Trp14ηH	i	Phe10ζH
e	Trp14ζ3H; Phe45ζH; Phe10δ2H		

[a] Taken from Breg et al. (1989).

The 2D NOESY spectra in the αH–αH region, where the NOE cross-peaks in the β-sheet region (residues 8–14) can be observed, show that the pressure-dissociated monomer is different from the thermal- or urea-denatured states. Figure 6 compares the NOESY spectra in the αH–αH region for the native state, the pressure-induced monomer state, the thermal-denatured state, and the urea-denatured state. The most important finding is that NOE cross-peaks between α-H of Glu9 and Arg13 occur even in the pressure-denatured form,

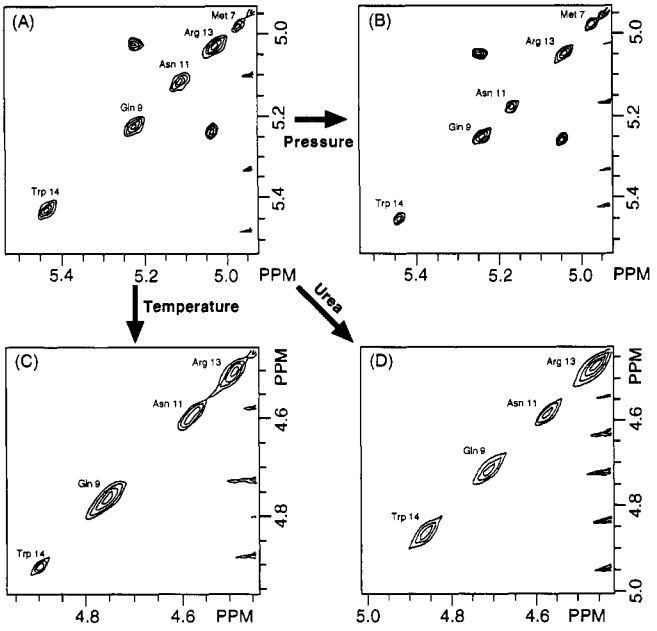

FIGURE 6: Comparison of an expanded region of NOESY spectra showing the αH–αH connection in the β-sheet region of the Arc repressor among the native state (A), the pressure-induced molten globule state (B), the thermally denatured state (C), and the urea-denatured state (D).

indicating the proximity of these two residues (Peng et al., 1993). By contrast, no NOEs are observed between α-H's of Glu9 and Arg13 in the NOESY spectra of the Arc repressor at 70 °C, nor in the presence of 7 M urea. This observation directly proves that Glu9 and Arg13 are no longer close to each other in the thermally or chemically denatured states.

Pressure-Induced Predissociated State of the Arc Repressor. As we mentioned in our preliminary note, we observed changes in 1D and 2D NMR spectra prior to pressure dissociation of the Arc repressor dimer and suggested the existence of a predissociated state. In the present study, we carried out additional 1D and 2D NMR experiments in order to prove the existence of the predissociated state.

The relative changes in the 1D spectra of both aromatic and aliphatic regions at 1 kbar with respect to 1 bar indicate that there must be some changes in the structure of the Arc repressor prior to its dissociation. In this pressure range, there is no dissociation of 1 mM Arc repressor dimer according to the fluorescence emission and polarization experiments (Silva et al., 1992).

Conclusive experimental evidence for the existence of a pressure-induced predissociated state of the Arc repressor comes from the 2D NOESY experiments in the αH–αH region of the β-sheet residues (residues 8–14) performed at high pressure. Figure 7 shows the NOESY spectra in the αH–αH region in the pressure range from 1 bar to 5 kbar at 20 °C. As expected, at 1 bar we observe a strong cross-peak between Glu9 and Arg13 (see Figure 7), which indicates the presence of the intermonomer β-sheet in the Arc repressor dimer as proposed by Berg et al. (1989, 1990). The increase in pressure to 500 bar does not produce any significant changes in the NOESY spectra, but they change drastically at 1 kbar. At 1 kbar, there appears an additional cross-peak between Glu9 and Trp14 and a cross-peak between Met7 and Glu9. Essentially the same NOESY spectrum persists at 1.5 kbar, but a 2 kbar only the cross-peak Glu9 and Arg13 persists. This cross-peak remains unchanged at pressures up to 5 kbar, i.e., in the pressure regime where the Arc repressor dissociates

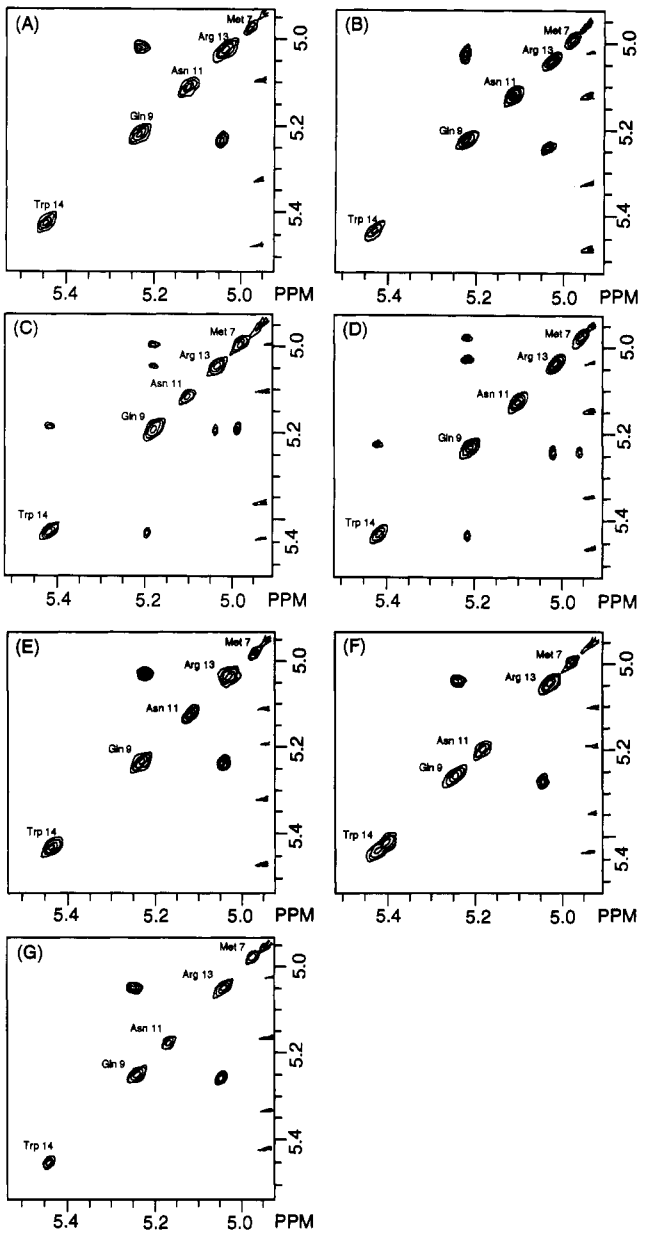

FIGURE 7: Expanded region of NOESY spectra at various pressures at 20 °C: 1 bar (A), 500 bar (B), 1 kbar (C), 1.5 kbar (D), 2.5 kbar (E), 3.5 kbar (F), 5.0 kbar (G).

into its molten globule monomers. This experimental evidence suggests that the conformation of the predissociated state could be intermediate between the antiparallel intermonomer β-sheet of the native dimer [see Breg et al. (1990)] and the intramolecular β-sheet of the molten globule monomer (Peng et al., 1993). Figure 8 shows the proposed conformations of the native dimer, predissociated state, and molten globule monomer of the Arc repressor. The structures of the predissociated state and the molten globule monomer were obtained from molecular dynamics calculations and energy minimizations. The predissociated dimer may be related to the transition state in the protein folding theory described by Creighton (1988), corresponding to a high-energy distorted form of the native conformation. Further increases in pressure cause the dissociation of the predissociated state into molten globule monomers.

Additional information on structural changes during pressure dissociation of Arc repressor can be obtained from the chemical shift values of the resolved α-H's of the β-sheet residues (Glu9, Asn11, Arg13, and Trp14). It is well

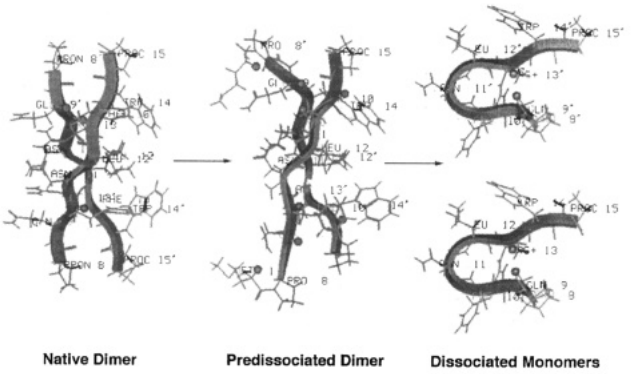

FIGURE 8: Proposed β-sheet structure of the Arc repressor in the native state, the predissociated state, and the dissociated molten globule state. The coordinates of the native dimer state were provided by R. Kaptein.

Table 2: Chemical Shift Values of α-Protons of Four Residues in the β-Sheet Region in the Various Conformational States

residue	native	predis (1 kbar)[a]	MG (4.5 kbar)[b]	thermally-D	urea-D	random coil[c]
Gln9	5.21	5.18	5.25	4.75	4.71	4.37
Asn11	5.11	5.10	5.17	4.60	4.57	4.75
Arg13	5.03	5.03	5.03	4.50	4.47	4.38
Trp14	5.43	5.42	5.44	4.90	4.87	4.70

[a] Predissociated state. [b] Molten globule state. [c] Taken from Wuthrich (1986).

established that a relationship exists between the α-CH chemical shifts of individual residues and the protein secondary structure. Table 2 lists the chemical shift values of α-H's for four residues located in the β-sheet region of the native state, predissociated state, molten globule state, thermally denatured state, urea-denatured state, and random-coil state. Inspection of differences in these chemical shift values indicates that these values are slightly dependent on pressure but markedly dependent on temperature or the presence of urea. It can be seen from Table 2 that the chemical shift values for α-H's of those four residues in the molten globule state are much greater than the corresponding random-coil values (Wuthrich, 1986), supporting the observation that these residues still maintain their β-sheet structure in the molten globule state (Wishart et al., 1992). However, the chemical shift values of Asn11 in the thermally denatured state and in the urea-denatured state are less than the corresponding random-coil value, indicating the disruption of the β-sheet in the thermally denatured state and the urea-denatured state.

Volume Change for the Arc Repressor Dissociation Reaction. There were two main reasons for determining the volume change for Arc repressor dissociation from the available 1D NMR data. First of all, Silva et al. (1992) pointed out that the large change in volume per mass of protein may be related to a high degree of interaction of buried amino acid side chains with the solvent upon dissociation. Therefore, a comparison of ΔV values determined by fluorescence and NMR data is of interest. Second, in the study for the unfolding of lysozyme (Samarasinghe et al., 1992), the different reaction volumes for unfolding of lysozyme could be correlated with the specific location of the residues in this protein. Since the NMR data allow us to determine ΔV's for different residues in the Arc repressor, the question of whether ΔV's are identical or vary with the location of the residue may provide additional information about the dissociation process.

Figure 9 shows the dissociation curves for two separate resonances at various pressures. For the resonance peaks

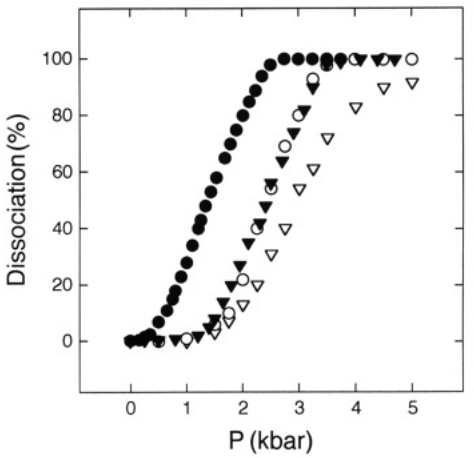

FIGURE 9: Pressure dissociation curves obtained from NMR spectra (1 mM) for resonances Trp14δ1H (○) and Tyr38ϵ2H (▽) and from fluorescence experiments for Trp14 (●) 20 μM and (▼) 1 mM.

Table 3: Volume Changes Calculated from Pressure Dissociation Curves

residue	Trp14δ1H[a]	Tyr38ϵ2H[a]	Trp14[b]
ΔV (mL/mol)	95 ± 10	72 ± 6	100 ± 4

[a] Resonance assignments according to Breg et al. (1989). [b] From fluorescence measurements (Silva et al., 1992).

corresponding to Trp 14δ1H [deconvoluted from resonances (b+c)] and Tyr38ϵ2H (which do not overlap with resonances of the dissociated state), the degree of dissociation was calculated according to

$$\alpha_P = 1 - I_P/I_0 \tag{3}$$

where I_P and I_0 refer to intensities of the corresponding resonance at pressures P and 1 bar, respectively.

The changes in the average fluorescence emission of Trp14 at two different protein concentrations are also shown in Figure 9. These dissociation curves shift to higher pressures by increases in protein concentration according to the expression given in the original reference (Silva et al., 1992). The changes in fluorescence emission overlap the changes in the NMR resonance of the δ1-protons of Trp14 with increasing pressure.

The volume changes for the dissociation process were derived from the transition curves in Figure 9 according to

$$\Delta V = -RT[\mathrm{d}(\ln K)/\mathrm{d}P] \tag{4}$$

$$K = \alpha_P{}^2 4C/(1 - \alpha_P) \tag{5}$$

where K and α_P refer to the dissociation constant and the degree of dissociation at pressure P, respectively. The ΔV values (Table 3) determined that the dissocation curves ranged from 72 to 100 mL/mol. The ΔV value of 95 mL/mol determined from the Trp14δ1 proton is in very good agreement with the value of 100 mL/mol determined by fluorescence experiments. The differences in the dissociation curves (Figure 9) and ΔV values for the Trp14 and Tyr38 residues suggest a low degree of cooperativity in the pressure denaturation of different regions of the Arc repressor.

It is interesting to note that the study of thermal denaturation of modified basic pancreatic trypsin inhibitor (RCOM-BPTI), where the disulfide bond 14–38 was reduced and the cysteinyl residues were protected by carboxymethylation, by Wuthrich et al. (1980) showed a different denaturation behavior for different individual residues. The authors concluded that the

cooperativity of the unfolding process for RCOM-BPTI is markedly reduced when compared to the unfolding behavior of BPTI. Similarly, the high-pressure NMR study of pressure-induced unfolding of lysozyme (Samarasinghe et al., 1992) concludes that there are statistically significant differences in ΔV values obtained for residues located in different regions of the protein.

CONCLUSIONS

In this study, high-resolution 1D and 2D NMR techniques have been used to investigate the conformational changes during the pressure-induced dissociation, temperature-induced denaturation, and chemical-induced denaturation of Arc repressor. The observed predissociation phenomena indicate the existence of an intermediate between the native dimer and the dissociated molten globule state of Arc repressor. The substantial line broadening and overlap of many resonances at pressures above 3.5 kbar indicate the existence of a molten globule structure of the dissociated monomer, in agreement with the fluorescence study. The NOEs between residues 9 and 13 in the molten globule monomer suggest that the molten globule contains an intramonomer β-sheet with a γ-turn. The substantial differences between spectra at 5 kbar, the spectra of the thermally denatured state at 70 °C, and the spectra of the urea-denatured state indicate that Arc repressor remains in the molten globule state up to 5 kbar.

In a general sense, the results of this study confirm our view that the use of pressure as an experimental variable allows a more controlled and less drastic perturbation of proteins than temperature or chemical agents.

ACKNOWLEDGMENT

We thank Professor Gregorio Weber and Ana Jonas for their constant support, encouragement, and helpful suggestions. We also thank Professor Robert T. Sauer (Massachusetts Institute of Technology) for providing the *E. coli* strain bearing the plasmid pTA200, and Professor R. Kaptein (University of Ulbrecht, The Netherlands) for providing his Arc dimer coordinates.

REFERENCES

Baum, J., Dobson, C. M., Evans, P. A., & Hanley, C. (1989) *Biochemistry 28*, 7–13.

Bax, A., & Davis, D. G. (1985) *J. Magn. Reson. 65*, 355–360.

Bax, A., Freeman, R., & Morris, G. J. (1981) *J. Magn. Reson. 42*, 164–168.

Bowie, J. U., & Sauer, R. T. (1989) *Proc. Natl. Acad. Sci. U.S.A. 86*, 2152–2156.

Braunschweiler, L., & Ernst, R. R. (1983) *J. Magn. Reson. 53*, 521–528.

Breg, J. N., Boelens, R., George, A. V. E., & Kaptein, R. (1989) *Biochemistry 28*, 9826–9833.

Breg, J. N., van Opheusden, J. H. J., Burgering, M. J. M., Boelens, R., & Kaptein, R. (1990) *Nature 346*, 586–589.

Brown, B. M., Bowie, J. U., & Sauer, R. T. (1990) *Biochemistry 29*, 11189–11195.

Creighton, T. E. (1988) *Proc. Natl. Acad. Sci. U.S.A. 85*, 5082–5086.

Dill, K. A., & Shortle, D. (1991) *Annu. Rev. Biochem. 60*, 795–825.

Goto, Y., & Kink, A. L. (1989) *Biochemistry 28*, 945–952.

Heremans, K. (1982) *Annu. Rev. Biophys. Bioeng. 11*, 1–21.

Jaenicke, R. (1987) *Prog. Biophys. Mol. Biol. 49*, 117–237.

Jaenicke, R. (1991) *Biochemistry 30*, 3147–3161.

Jonas, J. (1982) *Science 216*, 1179–1884.

Jonas, J. (1987) *NATO ASI Ser. 97*, 193–235.

Jonas, J., & Jonas, A. (1994) *Annu. Rev. Biophys. Biomol. Struct. 23*, 287–318.

Jonas, J., Peng, X., Koziol, P., Reiner, C., & Campbell, D. M. (1993) *J. Magn. Resn. 102B*, 299–309.

Kim, P. S., & Baldwin, R. C. (1982) *Annu. Rev. Biochem. 51*, 459–489.

Kim, P. S., & Baldwin, R. C. (1990) *Annu. Rev. Biochem. 59*, 631–660.

Knight, K. L., & Sauer, R. T. (1989) *Proc. Natl. Acad. Sci. U.S.A. 86*, 797–801.

Macura, S., Wuthrich, K., & Ernst, R. R. (1982) *J. Magn. Reson. 46*, 269–278.

Nemethy, G., & Printz, P. M. (1972) *Macromolecules 5*, 755–758.

Ohgushi, M., & Wada, A. (1983) *FEBS Lett. 164*, 21–24.

Paladini, A. A., & Weber, G. (1981) *Biochemistry 20*, 2587–2593.

Peng, X., Jonas, J., & Silva, J. L. (1993) *Proc. Natl. Acad. Sci. U.S.A. 90*, 1776–1780.

Phillips, S. E. V. (1991) *Curr. Opin. Struct. Biol. 1*, 89–98.

Ptitsyn, O. B. (1987) *J. Protein Chem. 6*, 273–293.

Ptitsyn, O. B., Pain, R. H., Semisotnov, G. V., Zerovnik, E., & Razgulyaev, O. I. (1990) *FEBS Lett. 262*, 20–24.

Rance, M., Sorenson, O. W., Bodenhauser, O., Wagner, G., Ernst, R. R., & Wuthrich, K. (1984) *Biochem. Biophys. Res. Commun. 117*, 479–485.

Rance, M., Bodenhausen, G., Wagner, G., Wuthrich, K., & Ernst, R. R. (1985) *J. Magn. Reson. 62*, 497–510.

Roder, H. (1989) *Methods Enzymol. 176*, 446–473.

Royer, C. A., Hinck, A. P., Loh, S. N., Prehoda, K. E., Peng, X., Jonas, J., & Markley, J. (1993) *Biochemistry 32*, 5222–5322.

Samarasinghe, S., Campbell, D. M., Jonas, A., & Jonas, J. (1992) *Biochemistry 31*, 7773.

Sauer, R. T., Krovatin, W., DeAnda, J., Youderian, P., & Susskind, M. M. (1983) *J. Mol. Biol. 168*, 699–713.

Shaka, A. J., & Freeman, R. (1983) *J. Magn. Reson. 51*, 169–173.

Silva, J. L., & Weber, G. (1993) *Annu. Rev. Phys. Chem. 44*, 89–113.

Silva, J. L., Miles, E. W., & Weber, G. (1986) *Biochemistry 25*, 5780–5786.

Silva, J. L., Villas-Boas, M., Bonafe, C. F. S., & Meirelles, N. C. (1989) *J. Biol. Chem. 264*, 15863–15868.

Silva, J. L., Silveira, C. F., Correia, A., Jr., & Pontes, L. (1992) *J. Mol. Biol. 223*, 545–555.

States, D. J., Haberkorn, R. A., & Ruben, D. J. (1982) *J. Magn. Reson. 48*, 286–292.

Susskind, M. M. (1980) *J. Mol. Biol. 138*, 685–713.

Vershon, A. K., Youderian, P., Susskind, M. M., & Sauer, R. T. (1985) *J. Mol. Biol. 260*, 12124–12129.

Vershon, A. K., Bowie, J., Karplus, T., & Sauer, R. T. (1986) *Proteins: Struct., Funct., Genet. 1*, 302–311.

Weber, G. (1987) *NATO ASI Ser. C 97*, 401–420.

Weber, G. (1993) *NATO ASI Ser., Ser. C 401*, 489–509.

Weber, G., & Drickamer, H. G. (1983) *Q. Rev. Biophys. 16*, 89–112.

Wishart, D. S., Sykes, B. D., & Richards, F. M. (1992) *Biochemistry 31*, 1647–1651.

Wuthrich, K. (1986) *NMR of Proteins and Nucleic Acids*, Wiley, New York.

Wuthrich, K., Roder, H., & Wagner, G. (1980) in *Protein Folding* (Jaenicke, R., Ed.) pp 549–564, Elsevier/North-Holland, Amsterdam.

Zagorski, M. G., Bowie, J. U., Vershon, A. K., Sauer, R. T., & Patel, D. J. (1989) *Biochemistry 28*, 9813–9825.

Zipp, A., & Kauzmann, W. (1973) *Biochemistry 12*, 4217–4228.